

PREDICTION OF PREGNANCY-INDUCED HYPERTENSION USING COHERENCE ANALYSIS

Kumari L. Fernando, V. John Mathews*

Dept of Electrical and Computer Engineering
University of Utah
Salt Lake City, UT 84112, USA

Michael W. Varner and Edward B. Clark

Depts of Obstetrics, Gynecology and Pediatrics
University of Utah,
Salt Lake City, UT 84132, USA

ABSTRACT

This paper presents a novel method to predict hypertensive disorders in pregnancy using coherence analysis. Previous studies suggest that there is inadequate secondary trophoblast invasion in hypertensive pregnancies implying that there are differences in the functional relationships between the maternal and fetal circulations. Magnitude squared coherence (MSC) is a function with values between 0 and 1 that indicates how well two waveforms correspond to each other in the frequency domain. The results presented in this paper using the MSC of maternal and fetal blood flow velocity waveforms indicate that in complicated hypertensive pregnancies its value is lower than in non-hypertensive controls. With additional validation, this method has the potential to provide an early test for hypertensive obstetric complications.

1. INTRODUCTION

Preeclampsia is a major cause of maternal mortality as well as perinatal morbidity and mortality. It is mainly characterized by hypertension and proteinuria. Preeclampsia affects as many as one in ten of all pregnancies if its milder forms are counted. Although clinical manifestations do not appear until the final three months, the foundations for preeclampsia are thought to be established in the first 10-12 weeks of gestation. Maternal complications due to preeclampsia are associated with the vascular system. Mothers are at risk for intravascular coagulation, bleeding, and organ failure. The intrauterine growth restriction, together with premature delivery, poses major threats to their fetuses leading to various degrees of morbidity and even death [1]. Long term follow up studies have demonstrated that babies who have suf-

fered intrauterine growth retardation are more likely to develop hypertension, coronary heart disease and noninsulin-dependent diabetes in adult life [2].

At present, the etiology of preeclampsia is unknown and there is no reliable way of predicting who will and who will not develop preeclampsia during early stages of pregnancy [3]. In this paper, we propose a method for predicting hypertensive disorders in pregnancy using coherence analysis of maternal and fetal arterial blood velocity waveforms estimated from Doppler ultrasound. The rest of this paper is organized as follows. The next section contains a description on the coherence analysis of fetal and maternal blood flows. Section 3 contains a brief introduction to the procedure for the acquisition of the blood flow velocity waveforms and preliminary results of employing coherence analysis on the acquired data. Finally, Section 4 contains the concluding remarks.

2. PREDICTION OF HYPERTENSION USING COHERENCE ANALYSIS

To provide the rationale for the method described in this paper, we briefly describe some of the relevant issues in placental-fetal development during early stages of pregnancy.

Before implantation, the cells of the early embryo separate into two types, the inner cell mass and the outer cells [1]. The inner cell mass becomes the fetus and its protective membranes, and the outer cells are collectively known as the trophoblast. The main purpose of the trophoblast is to form the placenta that juxtaposes the maternal and fetal circulations. A secondary function of the trophoblast is to engineer structural changes in the maternal blood vessels terminating in the placental bed, so that they can carry a substantial volume of blood to the placenta. These vessels are known as spiral arteries due to their coiled shape. The transformation of the spiral arteries takes place in two phases. During the primary trophoblast invasion within the first few weeks after implantation, the endometrial blood vessels are converted to

*This study was supported by an Innovative Research Grant from the Primary Children's Medical Center Foundation, Salt Lake City, Utah. The authors thank Nicolette T. C. Ursem, Piet C. Struijk and Juriy W. Wladimiroff for providing the ultrasound data used in the coherence analysis

the uteroplacental vessels. The secondary trophoblast invasion results in an increase in the vessel diameter and a decrease in the vessel wall thickness. Uterine arterial blood flow is the maternal input to the placental circulation system. About 85% of the total uterine flow supplies the placental circulation and the remaining 15% supplies the uterine musculature. Uterine artery supplies the nutrient and oxygen to the fetus via placenta from the mother. Fetal blood returns waste products to the placenta via the umbilical artery. When there is inadequate trophoblast invasion, spiral arteries remain narrow and result in reduced blood flow to the intervillous space reducing the supply of oxygen and nutrients to the fetus [4]. Evidence exists to suggest that there is inadequate trophoblast secondary invasion in pregnancies that later developed preeclampsia [1].

Based on the above description, we model the combined placental-fetal system as a dynamic system whose input and output signals are the uterine and umbilical arterial blood flows, respectively. Since there is evidence that absence or inadequacy of secondary trophoblast invasion contribute to the development of hypertensive disorders later in human pregnancy, we hypothesize that the functional relationship between the maternal and fetal blood flows are different in normotensive and hypertensive pregnancies. Furthermore, the secondary trophoblast invasion in the placental function typically occurs by the twelfth week of gestation. Therefore, it may be possible to identify hypertensive pregnancies through the analysis of maternal-fetal blood flows as early as the late-first or the early-second trimesters of pregnancy.

2.1. Coherence Analysis

In our work, we use the magnitude-square coherence (MSC) function [5] between the uterine and umbilical arterial blood flows to analyze the functional relationship between the two waveforms. Mathematically, the MSC function $|\gamma(\omega)|^2$ of the two waveforms $x(n)$ and $y(n)$ at frequency ω is given by

$$|\gamma(\omega)|^2 = \frac{|S_{xy}(\omega)|^2}{S_{xx}(\omega)S_{yy}(\omega)}, \quad (1)$$

where $S_{xy}(\omega)$ is the cross-spectrum, and $S_{xx}(\omega)$ and $S_{yy}(\omega)$ are the power spectra of the of $x(n)$ and $y(n)$, respectively.

The MSC is a function with values between 0 and 1 that indicates how well two waveforms correspond to each other in the frequency domain. If the two signals are linearly related, the coherence value is equal to one. If the two signals are uncorrelated, the coherence between the two signals is zero and it is less than one for nonlinearly related signals. Similarly, the coherence value is less than one whenever uncorrelated noise is present in the two signals.

Myatt [6] has stated that maternal oxidative stress in preeclamptic pregnancies can further attenuate the trophoblast invasion, and oxygen and nutrient delivery to the fetus. This

implies that, the relationship of maternal-fetal blood flow may be impaired in hypertensive pregnancies due to the changes in the maternal blood flow. Such changes will be most prominent in the frequency domain at the maternal heart rate, since the maternal blood flow drives the placental-fetal circulation system. Therefore, we hypothesize that in complicated hypertensive pregnancies such as those with preeclampsia, the MSC between maternal and fetal blood flow waveforms at the maternal heart rate is lower than in non-hypertensive pregnancies.

2.2. Selection of the Optimum Threshold Level

In this section, we briefly describe the process of selecting a single threshold value that can be employed to identify pregnancies at risk for subsequent hypertension from normotensive pregnancies using the square-root of the estimated MSC $\gamma(\omega_o)$ at the maternal heart rate ω_o . We select the threshold such that it maximizes a weighted sum of the sensitivity and the specificity of the algorithm. Sensitivity measures the proportion of the diseased subjects correctly identified by the test. Specificity of the test measures the proportion of the normal subjects correctly identified by the test. In order to select the threshold value that is applicable to all gestational ages, we first remove the gestational age dependent mean distribution from the estimated $\gamma(\omega_o)$ values. We denote the mean removed values of $\gamma(\omega_o)$ as $\tilde{\gamma}(\omega_o)$.

Let \mathcal{H}_o denote the null hypothesis that a given value of $\tilde{\gamma}(\omega_o)$ is within the hypertensive region and the alternative hypothesis \mathcal{H}_1 be that $\tilde{\gamma}(\omega_o)$ is within the normotensive region. Let $p_{norm}(\tilde{\gamma}(\omega_o))$ and $p_{hyp}(\tilde{\gamma}(\omega_o))$ be the probability density functions of $\tilde{\gamma}(\omega_o)$ for the normotensive and the hypertensive groups, respectively.

The conditional probability that $\tilde{\gamma}(\omega_o)$ belongs to the null hypothesis is denoted by

$$p(\tilde{\gamma}(\omega_o)|\mathcal{H}_o) = p_{hyp}(\tilde{\gamma}(\omega_o)). \quad (2)$$

Similarly, we define

$$p(\tilde{\gamma}(\omega_o)|\mathcal{H}_1) = p_{norm}(\tilde{\gamma}(\omega_o)) \quad (3)$$

as the conditional probability that $\tilde{\gamma}(\omega_o)$ belongs to the alternate hypothesis. Then, the threshold of detection $\tilde{\gamma}_{th}(\omega_o)$ is chosen such that the cost function

$$\mathcal{J} = w_1 \int_{-\infty}^{\tilde{\gamma}_{th}(\omega_o)} p_{hyp}(\tilde{\gamma}(\omega_o)) d\tilde{\gamma}(\omega_o) + w_2 \int_{\tilde{\gamma}_{th}(\omega_o)}^{\infty} p_{norm}(\tilde{\gamma}(\omega_o)) d\tilde{\gamma}(\omega_o), \quad (4)$$

is maximized, where w_1 and w_2 are positive weighting constants. We note that the first integral in the above expression

represents the sensitivity and the second integral defines the specificity of the algorithm.

At the optimum threshold level $\tilde{\gamma}_{th}(\omega_o)$,

$$\begin{aligned} \frac{\partial \mathcal{J}}{\partial \tilde{\gamma}_{th}(\omega_o)} &= w_{1hyp}(\tilde{\gamma}_{th}(\omega_o)) - w_{2norm}(\tilde{\gamma}_{th}(\omega_o)) \\ &= 0, \end{aligned} \quad (5)$$

implying that

$$w_{1hyp}(\tilde{\gamma}_{th}(\omega_o)) = w_{2norm}(\tilde{\gamma}_{th}(\omega_o)). \quad (6)$$

The solution to (6) provides the optimum threshold level $\tilde{\gamma}_{th}(\omega_o)$.

3. EXPERIMENTAL RESULTS

3.1. Data Acquisition

Doppler ultrasound blood velocity waveforms were collected at the Department of Obstetric and Gynecology, Academic Hospital Rotterdam-Dijkzigt, Rotterdam, The Netherlands. This study was approved by the Hospital Ethics Committee at the Erasmus University, The Netherlands.

No commercially available ultrasound machine has the capability of recording two waveforms simultaneously. For the preliminary studies, we assumed that there is no significant variation in the environmental, and fetal-umbilical and maternal-uterine waveform characteristics within short intervals of time. Therefore, blood velocity waveforms were recorded sequentially within a 5-minute interval. A total of 44 maternal-fetal data sets were collected during the 10th through the 22th week of gestation, of which 34 resulted in normal pregnancy outcome. Rest of the patients (10 data sets) developed the pregnancy-induced hypertension (PIH) subsequently. Transvaginal (5 MHz) and transabdominal (3.75 MHz) Doppler recording methods were used at 10-13 and 14-22 weeks of gestation, respectively. All Doppler studies were performed with the women in the semirecumbent position and during fetal apnea. The umbilical arterial velocity waveforms were obtained from the free floating loop of the umbilical cord. The angles of incidence of the ultrasound beams in the measurements were less than 20°. The sampling frequency of the blood velocity waveforms was 93.75 samples/sec and each waveform was recorded for approximately 20 seconds.

3.2. Results

We estimated the coherence values at the maternal heart rates for each pair of waveforms. First, the mean values of the maternal heart rate was estimated for each uterine-arterial waveform as the frequency corresponding to the peak of its amplitude spectrum. The amplitude spectrum was estimated as the absolute value of the Fourier transform estimated over the entire length of the blood velocity waveform.

The power spectrum and the cross-spectrum were estimated at the maternal heart rates as the average of the power spectra estimated over 16 or more 256-sample data segments. Each data segment was overlapped by 75% by the adjacent segment. The MSC values were estimated using (1).

Figure 1 displays the distribution of $\gamma(\omega_o)$, the square-root of the MSC function estimated at the maternal heart rate ω_o as a function of the gestational age. The open circles denote results for normotensive pregnancies and asterisks represent the corresponding results for hypertensive pregnancies. The average distribution of $\gamma(\omega_o)$ estimated as a

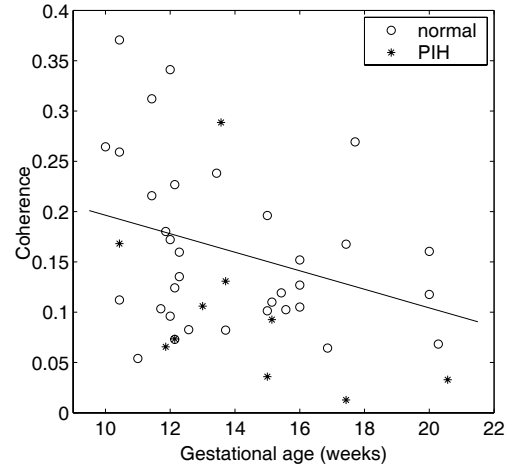


Fig. 1. Distribution of the square-root of the MSC function between maternal and fetal arterial blood flow at the maternal heart rate with gestational age.

function of the gestational age for normotensive pregnancies is shown by the solid line in Figure 1. This curve was obtained using a linear fit, and satisfies the relationship

$$\bar{\gamma}(\omega_o, \vartheta) = -0.0092\vartheta + 0.2885, \quad (7)$$

where $\bar{\gamma}(\omega_o, \vartheta)$ is the mean value of $\gamma(\omega_o)$ at the gestational age ϑ . Figure 1 demonstrates that the $\gamma(\omega_o)$ values estimated for pregnant women who subsequently developed PIH are in general well below the average for gestational age confirming the hypothesis that the average distribution of $\gamma(\omega_o)$ at maternal heart rate can be used as a marker for the identifying complicated pregnancies. In this work, we assumed that the distribution of the MSC function about its gestational age dependent mean value is the same for all gestational ages.

We now employ (6) for the selection of a threshold function to detect pregnancies that may later develop pregnancy. First, we estimated $\tilde{\gamma}(\omega_o)$ values by subtracting the gestational age dependent mean distribution from $\gamma(\omega_o)$ values. In our work, we assumed that $\tilde{\gamma}(\omega_o)$ in both the normotensive and hypertensive pregnancies belong to truncated

Gaussian distributions in the interval $[\tilde{\gamma}_{min}(\omega_o), \tilde{\gamma}_{max}(\omega_o)]$. The mean-removed MSC function at the maternal heart rate ranged from $\tilde{\gamma}_{min}(\omega_o) = -0.15$ to $\tilde{\gamma}_{max}(\omega_o) = 0.2$ for our data. The variance and mean values of $\tilde{\gamma}(\omega_o)$ were $\sigma_{norm}^2 = 0.0059$ and $\mu_{norm} = 0$, respectively, for normotensive pregnancies and $\sigma_{hyp}^2 = 0.0046$ and $\mu_{hyp} = -0.0764$, respectively, for hypertensive pregnancies. Figure 2 shows the distribution of the mean-removed coherence values and the threshold level for $w_1 = 5$ and $w_2 = 4$. In this case, the optimum threshold level was -0.0173 . The theoretically calculated sensitivity was 80.03% and the corresponding specificity was 58.11%. The experimentally evaluated sensitivity

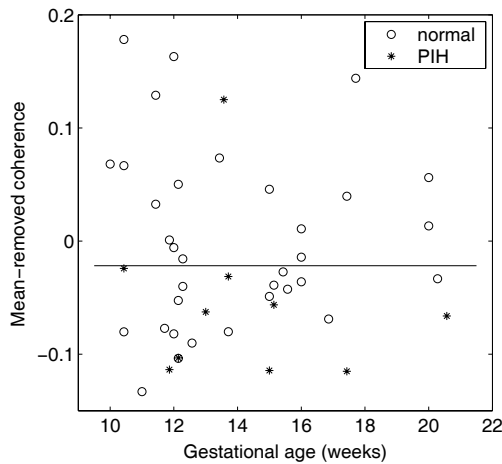


Fig. 2. Threshold level and coherence distribution.

and specificity of the test were 90% and 52.94%, respectively. With 22.73% prevalence of the condition in the acquired data, the positive predictive value of the test was 36% and the negative predictive value was 94.74%.

Finally, we compare our results with competing methods that employ Doppler ultrasound data (not presented). Martin and Schuchter *et al.* [7] presented results indicating that during early stages of pregnancy, the uterine-arterial pulsatility index (PI) increases in hypertensive pregnancies compared to the normotensive pregnancies. Ursem *et al.* [8] stated that in hypertensive pregnancies, the increased resistance to the fetal blood flow could be evaluated using the umbilical-arterial blood velocity variability. However, according to our analysis, there is no significant variation in uterine-arterial PI or umbilical-arterial blood velocity variability during 10-22 weeks of hypertensive pregnancies from normotensive pregnancies. Therefore, we believe that neither the PI nor the blood velocity variability are reliable indicators for subsequent development of preeclampsia.

4. CONCLUSIONS

Analysis of maternal arterial and fetal waveforms to predict subsequent development of hypertensive disorders in preg-

nancy is a novel concept. The preliminary analysis based on 44 sets of recordings shows that the absolute coherence between the two waveforms at maternal heart rate is smaller in pregnant women who subsequently developed hypertension than in women with normal pregnancies. The main advantages of our approach over the current diagnostic methods of hypertensive pregnancies are: (i) this method can be used to identify women at risk for hypertensive disorders at an earlier stage of pregnancy than currently possible, (ii) this method is non-invasive and simple to perform, and (iii) this method is highly sensitive. Therefore, this method can be used to screen pregnant women for additional tests and evaluation for potential onset of hypertensive disorders. Confirmation of these findings with additional recordings would allow the possibility of monitoring the pregnant women at risk for PIH with appropriate medical care.

5. REFERENCES

- [1] C. Redman and I. Walker, *Preeclampsia The Facts*, Oxford University Press, New York, New York, 1992.
- [2] R. Valdez, M. A. Athens, G. H. Thompson, B. S. Bradshaw, and M. P. Stern, "Birth weight and adult health outcomes in a biethnic population in the USA," *Diabetologia*, vol. 37, pp. 624–631, 1994.
- [3] A. C. Agudelo, R. Lede, and J. Belizan, "Evaluation of methods used in the prediction of hypertensive disorders of pregnancy," *Obstetrical and Gynecological Survey*, vol. 49, no. 3, pp. 210–222, March 1994.
- [4] R. E. Reiss, *Heart Disease in Infants, Children and Adolescents Including the Fetus and the Young Adult*, pp. 523–535, Williams and Wilkins, Baltimore, Maryland, 1995.
- [5] S. M. Kay, *Modern Spectral Estimation*, Prentice Hall, Englewood Cliffs, New Jersey, 1988.
- [6] L. Myatt, "Role of placenta in preeclampsia," *Endocrine*, vol. 19, no. 1, pp. 103–111, 2002.
- [7] A. M. Martin, R. Bindra, P. Curcio, and K. H. Nicolaides, "Screening for preeclampsia and fetal growth restriction by uterine artery Doppler at 11-14 weeks of gestation," *Journal of Ultrasound in Obstetrics and Gynecology*, vol. 18, pp. 583–586, 2001.
- [8] N. T. C. Ursem, E. B. Clark, W. C. J. Hop, B. B. Keller, and J. W. Wladimiroff, "Do heart rate and velocity variability derived from umbilical artery velocity waveforms change prior to clinical pregnancy induced hypertension," *Journal of Ultrasound in Obstetrics and Gynecology*, vol. 14, pp. 244–249, 1999.